Selenium-Containing Formate Dehydrogenase H from *Escherichia coli*: A Molybdopterin Enzyme That Catalyzes Formate Oxidation without Oxygen Transfer

Sergei V. Khangulov,*,‡ Vadim N. Gladyshev,‡,|| G. Charles Dismukes,§ and Thressa C. Stadtman‡

Laboratory of Biochemistry, National Heart, Lung, and Blood Institute, National Institutes of Health, Bethesda, Maryland 20892, and Hoyt Laboratory, Chemistry Department, Princeton University, Princeton, New Jersey 08544

Received September 3, 1997; Revised Manuscript Received December 18, 1997

ABSTRACT: Formate dehydrogenase H, FDH(Se), from *Escherichia coli* contains a molybdopterin guanine dinucleotide cofactor and a selenocysteine residue in the polypeptide. Oxidation of ^{13}C-labeled formate in ^{18}O-enriched water catalyzed by FDH(Se) produces $^{13}CO_2$ gas that contains no ^{18}O-label, establishing that the enzyme is not a member of the large class of Mo−pterin-containing oxotransferases which incorporate oxygen from water into product. An unusual Mo center of the active site is coordinated in the reduced Mo(IV) state in a square pyramidal geometry to the four equatorial dithiolene sulfur atoms from a pair of pterin cofactors and a Se atom of the selenocysteine-140 residue [Boyington, J. C., Gladyshev, V. N., Khangulov, S. V., Stadtman, T. C., and Sun, P. D. (1997) *Science 275,* 1305−1308]. EPR spectroscopy of the Mo(V) state indicates a square pyramidal geometry analogous to that of the Mo(IV) center. The strongest ligand field component is likely the single axial Se atom producing a ground orbital configuration Mo(d_{xy}). The Mo−Se bond was estimated to be covalent to the extent of 17−27% of the unpaired electron spin density residing in the valence 4s and 4p selenium orbitals, based on comparison of the scalar and dipolar hyperfine components to atomic ^{77}Se. Two electron oxidation of formate by the Mo(VI) state converts Mo to the reduced Mo(IV) state with the formate proton, H_f^+, transferring to a nearby base Y^-. Transfer of one electron to the Fe_4S_4 center converts Mo(IV) to the EPR detectable Mo(V) state. The Y^- is located within magnetic contact to the [Mo−Se] center, as shown by its strong dipolar ^1H_f hyperfine couplings. Photolysis of the formate-induced Mo(V) state abolishes the ^1H_f hyperfine splitting from YH_f, suggesting photoisomerization of this group or phototransfer of the proton to a more distant proton acceptor group A^-. The minor effect of photolysis on the ^{77}Se-hyperfine interaction with [^{77}Se] selenocysteine suggests that the Y^- group is not the Se atom, but instead might be the imidazole ring of the His141 residue which is located in the putative substrate-binding pocket close to the [Mo−Se] center. We propose that the transfer of H_f^+ from formate to the active site base Y^- is thermodynamically coupled to two-electron oxidation of the formate molecule, thereby facilitating formation of CO_2. Under normal physiological conditions, when electron flow is not limited by the terminal acceptor of electrons, the energy released upon oxidation of Mo(IV) centers by the Fe_4S_4 is used for deprotonation of YH_f and transfer of H_f^+ against the thermodynamic potential.

Molybdenum-containing enzymes comprise a group of proteins differing in structure and function that catalyze a number of key metabolic steps in the metabolism of sulfur, carbon, and nitrogen compounds. They serve as catalysts in the hydroxylation of aromatic heterocycles and as oxygen atom transfer agents to/from organic and inorganic substrates. In all known molybdoenzymes except nitrogenases, Mo is bound to a pterin−dithiolene structure termed a molybdopterin (*1*−*3*). Three Mo−pterin enzymes that have been characterized by X-ray crystallography are aldehyde oxidoreductase from *Desulfovibrio gigas*, DMSO reductase from *Rhodobacter sphaeroides*, and formate dehydrogenase from *Escherichia coli* (*4*−*6*). All three enzymes share a common structural element in which the Mo atom is coordinated to dithiolene ligands of two Mo−pterins. This structural pattern was first discovered in the tungsten-containing enzyme, aldehyde:ferredoxin oxidoreductase from *Pyrococcus furiosus* (*7*).

Selenium- and molybdenum-containing formate dehydrogenase H, FDH(Se),[1] and hydrogenase 3 are components of the *E. coli* formate hydrogen lyase complex which decomposes formate to carbon dioxide and hydrogen under anaerobic conditions in vivo (*8*). FDH(Se) was purified (*9*), and the enzyme was shown to contain a selenocysteine residue (*10*) encoded by the UGA codon (*11*), molybdenum, the FeS center (*9*), and a molybdopterin guanidine dinucleotide (*9*, *12*), Chart 1.

The enzyme is extremely sensitive to oxygen in dilute solutions, particularly after reduction with substrate (*9*).

* To whom correspondence should be addressed. Current address: Chemistry Department, Hoyt Laboratory, Princeton University, Princeton, NJ 08544. E-mail: khang@chemvax.princeton.edu.

‡ NIH.

§ Princeton University.

|| Current address: Department of Biochemistry, University of Nebraska, Lincoln, NE 68588.

[1] Abbreviations: FDH(Se), selenium-containing formate dehydrogenase H; FDH(S), SeCys140Cys mutant formate dehydrogenase; EPR, electron paramagnetic resonance.

S0006-2960(97)02177-6 CCC: $15.00
Published on Web 02/18/1998

Chart 1: Proposed Coordination of Mo to the Dithiolene Ligands of H_4-Molybdopterin Guanine Dinucleotide in FDH(Se) (*12*)

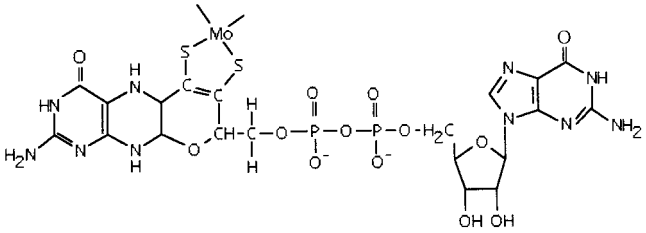

The first evidence for direct ligation of a Se atom to a Mo center was reported in 1994 for nicotinic acid hydroxylase from *Clostridium barkeri* and for FDH(Se) from *E. coli* (*13*, *14*). The nicotinic acid hydroxylase contains a Se atom in the form of an unidentified dissociable cofactor (*15*, *16*) whereas FDH(Se) contains Se in the form of a selenocysteine residue at position 140 (*10*, *11*). The activity of the (SeCys)-140Cys mutant enzyme was only 0.3% that of the wild-typeenzyme (*17*) and a (SeCys)140Ser mutant was inactive (*18*).

Most known Mo−pterin containing enzymes are oxotransferases catalyzing transfer of an oxygen atom from water to product (*19*−*22*), eq 1. Formate dehydrogenase might also

$$X + H_2O \rightleftharpoons XO + 2e + 2H^+ \quad (1)$$

be considered to be a "classical" oxotransferase if the direct product of formate oxidation is bicarbonate (eq 2a) whereas if carbon dioxide is the actual product (eq 2b) then this molybdoenzyme is an exception in terms of reaction mechanism.

$$H_2O + HCOO^- \xrightarrow{\text{FDH(Se)}} HCO_3^- + 2e + 2H^+ \quad (2a)$$

$$HCOO^- \xrightarrow{\text{FDH(Se)}} CO_2 + 2e + H^+ \quad (2b)$$

An EXAFS study of FDH(Se) in different oxidation states failed to detect any oxo−Mo species analogous to those present in many molybdoenzymes (*23*). Crystallographic analysis of FDH(Se) in both reduced, Mo(IV), and oxidized, Mo(VI), states revealed that the Mo ion is ligated to four *cis*-dithiolene sulfur atoms of the two bound Mo−pterin guanine dinucleotides and also to the Se of SeCys140 (*6*). The coordination geometry of the Mo(IV) center is close to a square pyramid with the four S in equatorial sites and the Se at the axial position. Oxidation of the Mo(IV) state is accompanied by large structural distortions of the coordination sphere due to insertion of a sixth ligand, presumably OH^-.

The presence of only one Se atom in FDH(Se) provides a unique opportunity for selective ^{77}Se-labeling of the Se-ligand and evaluation of the ^{77}Se-hyperfine interaction with the paramagnetic Mo(V) center. In the present study we have used the hyperfine interaction of the ^{77}Se-atom with the central Mo(V) ion as an extremely sensitive probe of the electronic- and coordination structures of the central Mo(V) ion and a measure of the covalent bonding between metal ion and Se. Using mass spectrometric analysis of $^{13}CO_2$ formed by oxidation of ^{13}C-labeled formate in ^{18}O-enriched water we have shown that carbon dioxide rather than bicarbonate is the primary product of formate oxidation.

MATERIALS AND METHODS

Purification of Enzymes. *E. coli* strain FM911 containing plasmid pFM20 was cultured as described previously (*9*) and was used as a source of SeCys-containing FDH(Se). For the ^{77}Se-labeled enzyme this strain was cultured in the presence of 1 μM [^{77}Se]selenite. *E. coli* mutant strain WL31153 containing plasmid pFM210 (*18*) was grown as described previously (*24*) and was used as a source of mutant formate dehydrogenase, FDH(S), in which SeCys140 was replaced with Cys. FDH(Se) and FDH(S) used for EPR experiments were isolated from 300 g of cells by a modified procedure as described (*24*). All procedures involving FDH-(Se) and FDH(S) purification, enzyme activity measurements, and sample preparation were performed in a nitrogen atmosphere in the presence of 1−4% hydrogen in the National Institutes of Health Anaerobic Laboratory, operating below 1 ppm of oxygen (*25*). All solutions were stored in the Anaerobic Laboratory for at least 48 h and then purged for 15 min with oxygen-free argon prior to use. Benzyl viologen dependent formate dehydrogenase activities of FDH(Se) and FDH(S) were monitored as described (*24*). Enzyme solutions of FDH(Se) in 3 mM sodium azide and 25 mM MES, pH 6.0, were concentrated to ca. 10 mg protein/mL using a 50 mL Amicon concentration cell and Centricon-30 microconcentrators.

Mass Spectrometry. Samples for analysis of the isotope composition of CO_2 gas released upon enzymatic oxidation of ^{13}C-labeled formate in ^{18}O-enriched water were prepared using two anaerobic solutions. The first solution, D1, contained 11.1% $H_2{}^{18}O$, 22.2 mM sodium ^{13}C-formate, 2.2 mM benzyl viologen, 3.3 mM NaN_3, and 11.1 mM MES, pH 6.5. The second solution, D2, contained 26 μM FDH-(Se), 3.0 mM NaN_3, and 25 mM MES, pH 6.5. Both solutions were frozen under strictly anaerobic conditions in the form of small droplets in liquid nitrogen.

The frozen droplets of D1 and D2, weighing 132 and 24.2 mg, respectively, were placed in mass-spectrometric cell and kept under vacuum for 10−15 min at 200 K. After the valve was sealed, the cell was placed in a water bath at 25 °C to melt the droplets. The reaction was initiated by fast mixing with a small magnetic bar at the bottom of the cell. Almost instantly the reaction mixture turned a violet color due to reduction of benzyl viologen, and vigorous CO_2 release was observed. After 10 s the sample was frozen in liquid nitrogen and then the cell was transferred to a dry ice/ethanol bath followed by mass spectral analysis of the released gas by thermal desorption as described (*26*).

Preparation of EPR Samples. Formate-treated enzyme samples were prepared by 5−10 s incubation of the enzyme (100 μL) with 20 mM sodium formate followed by freezing in liquid nitrogen. In a few cases indicated in the text, sodium ^{13}C-formate (^{13}C, 99%) and ^{2}H-formate, $DCOO^-$ (D, 98%) from Cambridge Isotopes were used for preparation of formate-treated FDH(Se) samples. The D_2O substitution of FDH(Se) was performed by dilution of 100 μL of concentrated enzyme (40 mg/mL) in 4 mL of 25 mM MES buffer, pH 6.0, containing 3 mM sodium azide in D_2O (98 %, Isotec), followed by concentration of the protein on a

Centricon-30 microconcentrator (Amicon). Dithionite-reduced samples of FDH were prepared by incubation of the protein in the presence of 10 μM methyl viologen, 50 mM Tris−HCl, pH 8.5 with 5 mM sodium dithionite for 30 min at 0 °C.

Oxygen Sensitivity of the FDH(Se). In an experiment similar to those described by Gladyshev et al. (*27*), 0.5 mg samples of FDH(Se) in 100 μL of 25 mM MES, pH 6.0, containing 3 mM NaN_3, and 20 mM formate (sample 1) or no formate (sample 2), were prepared under strictly anaerobic conditions and then incubated for 1 h at 4 °C aerobically outside of the Anaerobic Laboratory. Then both samples were flushed with argon, incubated overnight in the Anaerobic Laboratory at 4 °C, and transferred to quartz tubes for EPR measurement. Assay of aliquots from samples 1 and 2 for formate dehydrogenase activity revealed that the formate-treated FDH(Se) was completely inactive in the BV-dependent oxidation of formate, whereas the formate-free FDH(Se) retained 95% of the initial activity.

Light Sensitivity of Mo(V) of the FDH(Se). Enzyme samples were illuminated in the helium cryostat using a halogen lamp (150 W) filtered through a $CuSO_4$ solution used as a heat-filter. Prior to the EPR measurements the samples were placed in a dry ice/ethanol mixture and kept in darkness for 10 min.

EPR Measurements. EPR spectra were recorded using a Bruker X-band ESP-300 spectrometer operating with microwave rectangular TE_{102} cavity (ER 4102 ST) and equipped with a 5352B microwave frequency counter (Hewlett-Packard). Magnetic field calibration was made with α,α,α-diphenyl-β-picrylhydrazyl as a *g*-factor standard. The frequency of magnetic field modulation was 100 kHz. Except where noted, EPR spectra of the Mo(V) species were recorded at 130 K using 2.5 G modulation amplitude and microwave power *P* of 15.2 mW. The EPR spectra of iron−sulfur centers were recorded at 43 K and 5.0 G modulation amplitude. EPR measurements at 130 K and below 77 K were performed using flow nitrogen and helium cryostats, respectively.

EPR simulations employed the QPOW computer program written by Nilges (*28*). The program permits simulation of a powder EPR spectrum of particles with an anisotropic **g**-tensor (*g*) and electron spin $S = {}^1/_2$ coupled by an anisotropic hyperfine interaction (*A*) with the nucleus spin $I > 0$.

An estimation of the spin concentration was made by numerical integration of the unsaturated EPR spectra and by comparison with a Cu−EDTA standard. To compare concentrations of paramagnetic species detected at different temperatures and microwave powers the double integrals were multiplied by $T/(g_pP^{1/2})$, where g_p is the *g* factor (*29*). The EPR spectra of Mo(V) species are a superposition of a minor EPR signal from ^{95,97}Mo isotopes (25.2% natural abundance), having nuclear spin $I = {}^5/_2$, and a stronger signal from Mo isotopes having $I = 0$ (natural abundance 74.7%). Therefore, to estimate the total content of Mo(V) species the double integral corresponding to the $I = 0$ species was multiplied by the correction factor of 1.34.

RESULTS

Carbon Dioxide Is the Product of Formate Oxidation. Mass-spectrometric analysis of the isotopic composition of CO_2 gas, released upon enzymatic oxidation of [^{13}C]formate in ^{18}O-enriched water, was performed to determine whether CO_2 is the direct oxidation product of the reaction (eq 3a)

$$H^{13}COO^- + 2\ BV_{ox} \xrightarrow{FDH(Se)} {}^{13}CO_2 + H^+ + 2\ BV_{red} \quad (3a)$$

or if it is produced indirectly by dehydration of bicarbonate (eq 3b) (where BV is benzyl viologen).

$$H^{13}COO^- + H_2{}^{18}O + 2\ BV_{ox} \xrightarrow{FDH(Se)} H_2{}^{13}COO^{18}O + H^+ + 2\ BV_{red}$$
$$\Big\Downarrow \text{FDH(Se) ?}$$
$$^{13}CO^{(18)}O + H_2{}^{(18)}O \quad (3b)$$

A ratio of 0.063 for [$^{13}C^{16}O^{18}O$]/[$^{13}C^{16}O^{16}O$] is predicted for formation of ^{18}O-labeled CO_2 by reaction 3b in 9.4% $H_2{}^{18}O$ water abundance. The carbon dioxide gas trapped after 10 s after initiation of the reaction at pH 6.5 was exclusively the $^{13}C^{16}O^{16}O$-isotopomer and no $^{13}C^{16}O^{18}O$- or $^{13}C^{18}O^{18}O$-isotopomers were detected. At a higher pH value, 7.5, a ratio of 0.01 for [$^{13}C^{16}O^{18}O$]/[$^{13}C^{16}O^{16}O$] was detected at 10 s after initiation of the reaction. After 35 min, the content of the ^{18}O-enriched ^{13}C-carbon dioxide ([$^{13}C^{16}O^{18}O$]/[$^{13}C^{16}O^{16}O$]) was increased up to 9.0% which is close to the maximum possible value of 9.4%. This slow increase undoubtedly is due to a secondary ^{16}O/^{18}O-exchange process, $^{13}CO_2 + H_2{}^{18}O \leftrightarrow H_2{}^{13}COO^{18}O$, which is accelerated at alkaline pH values. These results indicate that, in accordance with eq 3a, water is not involved in the oxidation of formate by FDH(Se) and CO_2 is the initial product of the catalytic reaction.

Formate Induces a Mo(V) EPR Signal in FDH(Se),"2.094" Signal; ^{95,97}Mo and ^{77}Se Hyperfine Structure. As-isolated FDH(Se) is EPR silent at $T > 80$ K; treatment of the enzyme with formate (20 mM) induces the EPR signal presented in Figure 1a.

The signal is stable and was observed without significant decrease in amplitude even after 12 h of incubation with formate at 4 °C under strictly anaerobic conditions. Its line shape does not depend on pH over the range from 6.0 to 8.5 (not shown). At higher gain, a number of satellite peaks are observed (bars in Figure 1b). These features are similar to the ^{95,97}Mo hyperfine structure of the Mo(V) EPR signal of nicotinic acid hydroxylase (*13*) and allow estimation of the molybdenum hyperfine constants, $(A_{zz}, A_{xx}, A_{yy}) = (39.2 \times 10^{-4}, 23.6 \times 10^{-4}, 23.6 \times 10^{-4}\ cm^{-1})$, Table 1. This Mo(V) EPR signal has a $g_{\|}(g_z)$ value of 2.094 and a $g_\perp$ component of about 2.0 and is denoted in this paper as the "2.094" signal. A set of control experiments showed that azide, which is required to preserve enzyme activity during isolation, does not affect the line shape or the amplitude of the "2.094" EPR signal.

The "2.094" EPR signal also is induced by sodium dithionite, but the amplitude of the dithionite-induced signal is about 20% of that detected in formate-treated FDH(Se). The identical line shapes of the dithionite- and formate-induced signals suggest that neither formate nor a product of its degradation is involved in direct coordination to Mo-(V).

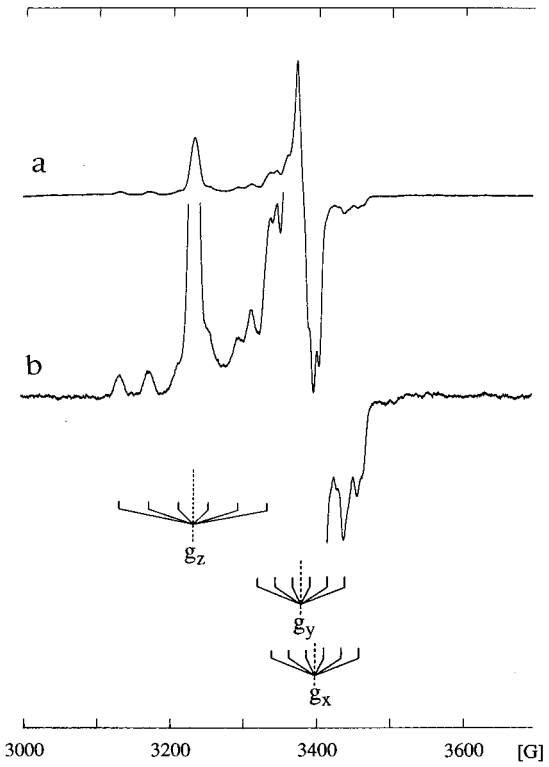

FIGURE 1: EPR spectra of formate-treated FDH(Se) at 130 K. (a) The sample has been frozen after incubation of FDH(Se) with 20 mM formate for 10 s. (b) This is the same spectrum as in part a but at higher gain. The g_z, g_y, and g_x components of Mo(V) species with $I = 0$ are marked by dashed lines. The hyperfine features from Mo(V) isotopes with $I = {}^5/_2$ are marked by short sticks.

Table 1: The *g*-Factors and the Absolute ^{95,97}Mo, ^{1}H, and ^{77}Se Hyperfine Values ($\times 10^{-4}$ cm^{-1}) for Mo(V)

	"2.094"			light-induced "2.106"		
EPR signal	*z*	*y*	*x*	*z*	*y*	*x*
g	2.094	2.001	1.990	2.106	2.002	1.990
^{95,97}Mo	39.2	23.6	23.6	39.0	nd[a]	nd
^{77}Se	4.4	25.0	80.1	4.7	25.0	90.0
^{1}H	2.5	6.3	7.0	<0.1	<0.1	<0.1

[a] No data.

Sensitivity of the Mo(V) Center to Oxygen. At low protein levels and under anaerobic conditions FDH(Se) is rapidly inactivated in pH 6.0 buffer solutions by traces of dissolved oxygen (*27*). However concentrated (3−6 mg protein/mL) formate-free enzyme solutions can be exposed to air for 1 h without appreciable loss of catalytic activity.

Likewise, the ability to generate the "2.094" EPR signal upon addition of substrate is retained by enzyme incubated aerobically for 1 h in a formate-free solution at a high protein concentration. Assays of enzyme samples (0.5 mg/100 μL prepared as described in the Materials and Methods showed that sample 2, exposed to air in the absence of substrate, retained almost full catalytic activity, and after reaction with 20 mM formate for 10 s the "2.094" EPR signal was detected. Following this reaction with formate, exposure to aerobic conditions for 10 s led to inactivation of the FDH-(Se) and eliminated the "2.094" signal. A new minor Mo-(V) EPR signal, characteristic of the autooxidized enzyme (not shown) was detected after the reduced sample had been transferred back to anaerobic conditions. The catalytic activity of enzyme, exposed to air for 1 h in the presence of 20 mM formate, sample 1, was only 5% that of the formate-free sample 2. Moreover, sample 1 failed to generate the "2.094" signal when more formate was added. Thus the loss of catalytic activity due to exposure of substrate reduced enzyme to oxygen occurs in parallel with loss of ability to generate the Mo(V) type "2.094" EPR signal upon addition of formate.

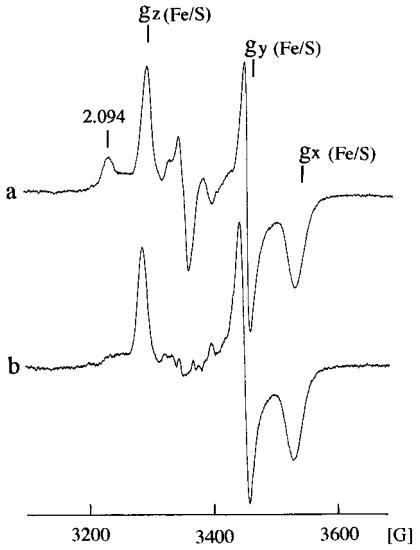

FIGURE 2: (a) EPR spectrum of formate-treated FDH(Se) at 42 K. FDH(Se) was incubated with 20 mM formate for 10 s and then frozen. Microwave power P is 64 mW. (b) EPR signal of Fe_4S_4 clusters obtained after subtraction of the Mo(V) "2.094" signal from spectrum a.

Table 2: Relative Concentrations of Mo(V) and Reduced Fe_4S_4 Centers in Formate-Treated FDH(Se) at Different pH Values

pH	6.0	6.5	7.0	8.0
[Mo(V)]/[enzyme]	0.5	0.6	0.7	0.3
[Fe/S]/[enzyme]	0.4	0.6	0.6	0.4
[Mo(V)]/[Fe/S]	1.3	1.0	1.2	0.75

The EPR Signal of the Fe_4S_4 Cluster. An EPR signal from the reduced iron sulfur cluster could be detected in formate- and dithionite-reduced FDH(Se) at $T < 55$ K. This signal (EPR signal "1.95") with *g*-factors g_z, g_y, g_x, and g_{av} of 2.04_5, 1.95_7, 1.84_0, and 1.94_7, respectively, is shown in Figure 2.

No other Fe_4S_4 EPR signal was observed for formate- or dithionite-reduced FDH(Se) over a range of temperatures from 10 to 55 K. An identical "1.95" EPR signal was observed in formate-treated FDH(^{77}Se) and in dithionite-reduced (SeCys)140Cys mutant enzyme, indicating that the Se atom of SeCys140 is not a part of the Fe_4S_4 cluster, nor do Se atoms replace the sulfido bridges in the iron−sulfur cluster. Indeed, if replacement of a terminal or bridging S atom in the Fe_4S_4 cluster by Se occurred, it would change significantly the EPR signal (*30*−*32*).

The line shapes of the "2.094" and "1.95" signals do not depend on pH in the range from 6 to 8. The concentrations of the Mo(V) and reduced Fe_4S_4 centers presented in Table 2 were determined by integration of the formate-induced "2.094" and "1.95" signals, respectively.

These data show that the Mo(V) species account for the majority of centers. Moreover, in the absence of a terminal acceptor, the two-electron oxidation of one formate molecule

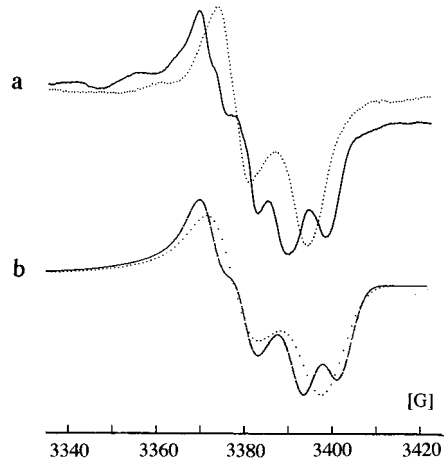

FIGURE 3: Proton hyperfine features of the "2.094" signal in the $g \approx 2$ region. The EPR spectra given in solid lines in parts a and b are the "2.094" signal and the simulation, respectively. The dotted spectra in parts a and b are the EPR signal "2.094(D)" and the simulation, respectively. The simulation parameters are given in Table 1.

results in the formation of approximately equal amounts of the Mo(V) center and the reduced Fe_4S_4 cluster.

The Formate Hydrogen Atom Is Transferred to a Site Y⁻ That Is Coupled to the Mo(V) Center. Inspection of the $g \approx 2$ region of the "2.094" signal reveals a set of resolved peaks (Figure 3).

Experiments with deuterioformate ($DCOO^-$, ^{2}H-formate) and D_2O indicate that these features are derived from a hyperfine interaction of the Mo(V) center with the formate-derived proton. Indeed, a new signal, termed the "2.094-(D)" signal appears when FDH(Se) is incubated for 5 s with ^{2}H-formate. This new signal is characterized by a nearly axial **g**-tensor (g_z, g_y, g_x) = (2.094, 2.001,1.990), Table 1, and a loss of ^{1}H-hyperfine features in the $g \approx 2$ region (Figures 3 and 4).

In addition, ^{2}H-formate considerably decreases the line width of the g_z component from 13.2 to 10.5 G (half-width). This narrowing occurs because the deuteron has a 6.5-fold smaller magnetic moment than a proton therefore in ^{2}H-formate-treated FDH(Se) the unresolved ^{1}H-hyperfine splitting contributing to the line width of the g_z-component is substituted by much weaker ^{2}H-hyperfine splitting. Because the ^{1}H hyperfine features of the "2.094" signal are due to hyperfine interaction with a $HCOO^-$-derived proton, this proton is denoted H_f^+; by analogy, the deuteron abstracted from ^{2}H-formate is called D_f^+.

H_f^+ (or D_f^+) is water-exchangeable. Indeed, the line shape of the ^{2}H-formate-induced signal depends on the time of incubation with ^{2}H-formate. FDH(Se) treated with ^{2}H-formate for less than 5 s exhibited the "2.094(D)" signal only, whereas after 30 s the observed signal was approximately a 1:1 superposition of the "2.094(D)" and "2.094" signals. After 5 min the "2.094(D)" was completely converted into "2.094" signal.

The rate of the exchange reaction is strongly pH-dependent. At pH 8.5, no detectable conversion of the ^{2}H-formate-induced "2.094(D)" signal into the "2.094" signal was observed after 30 s incubation of FDH(Se) in H_2O with ^{2}H-formate. After about 300 s the ^{2}H-formate-induced "2.094(D)" signal was converted into a 1:1 superposition of the "2.094(D)" and "2.094" signals.

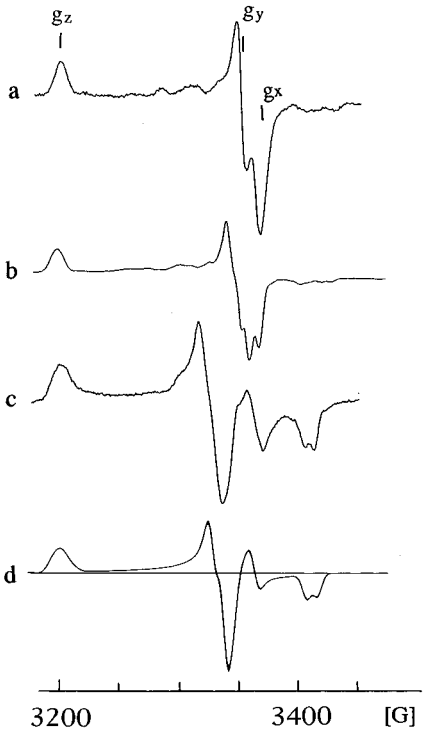

FIGURE 4: Comparison of formate-induced EPR signals of FDH-(Se) and FDH(^{77}Se). Spectra a and b were detected after 10 s incubation of FDH(Se) with 20 mM ^{2}H-formate and ^{1}H-formate, respectively. Spectrum c was detected after 10 s incubation of FDH(^{77}Se) with 20 mM ^{1}H-formate. Spectrum d is a simulation of the EPR spectra c. Simulation parameters are shown in Table 1.

The involvement of water in the proton exchange is demonstrated in experiments with D_2O. FDH(Se) in D_2O (pH 6.5) frozen immediately after addition of ^{1}H-formate exhibited only the "2.094" signal. If the FDH(Se) in D_2O was incubated with ^{1}H-formate for a longer period of time (>30 s) the "2.094" became smaller and growth of "2.094-(D)" was observed. The ^{1}H-hyperfine constants found by spectral simulations of the "2.094" and "2.094(D)" signals (Figures 3 and 4a,b) are listed in Table 1.

^{77}Se Hyperfine Structure of the Mo(V) EPR Signal. The ^{77}Se-substitution essentially transforms the $g \approx 2$ region of the "2.094" signal and increases the half-width of the g_z component from 13.2 to 17.9 G. A comparison of the formate-induced signals from FDH(Se) and FDH(^{77}Se) is shown in Figure 4 b,c. The absolute values of the (^{77}Se)-hyperfine tensor, obtained from simulation of the "2.094(^{77}-Se)" signal in Figure 4c, are given in Table 1. These ^{77}Se hyperfine values are much larger than the values, obtained for $[MoO(^{77}SePh)_4]^-$ (*33*), (A_{zz}, A_{yy}, A_{xx}) = (16.9×10^{-4}, -15.0×10^{-4}, -15.0×10^{-4} cm^{-1}), where Mo(V) is coordinated to four selenium atoms in, presumably, a planar configuration.

Light Sensitivity of the "2.094" Signal. Formate-treated samples of FDH(Se) exhibit a light-dependent behavior, which in many respects is analogous to the light-dependent phenomena of the [Ni−Fe]-hydrogenases (*34*−*36*).

The EPR spectrum of formate-treated, dark-adapted FDH-(Se) at 15 K (see Materials and Methods) is shown in Figure 5b.

This spectrum is a superposition of two EPR signals from the "2.094" Mo(V) and "1.95" Fe_4S_4 species. The spectrum presented in Figure 5a is observed after 5 s illumination of

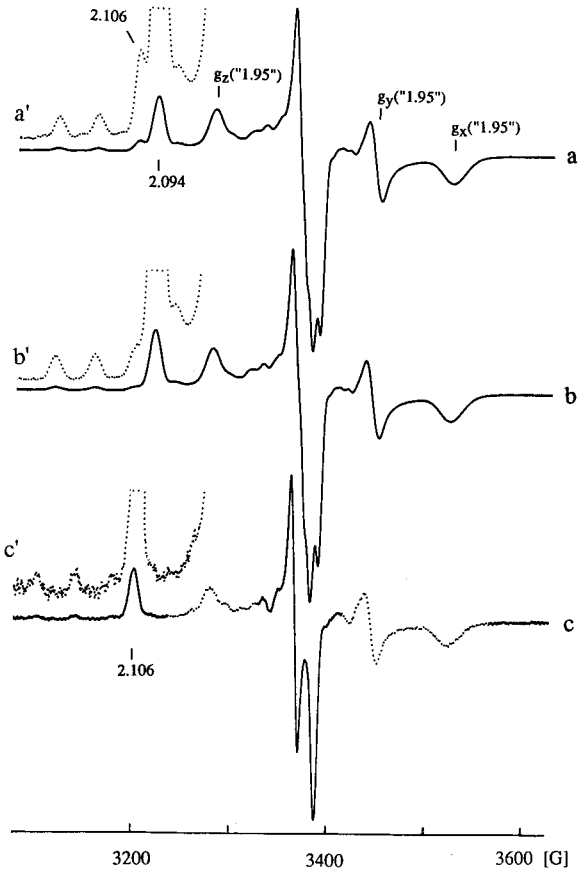

FIGURE 5: Effect of low-temperature illumination on EPR signals of formate treated FDH(Se) (solid lines). Spectrum b was obtained from a "dark adapted" sample (see Materials and Methods). Spectrum a was obtained from the sample illuminated for 5 s at 35.9 K. Spectrum c is a difference c = a(light) − 0.9 × b(dark); for plotting purposes spectrum c was multiplied by 7.2. The spectra a′, b′, and c′ (dotted lines) were obtained after an expansion by 8 × of a, b, and c, respectively. Spectra were accumulated at T = 35.9 K and P = 0.81 mW.

the FDH(Se) sample at 15 K. The most pronounced effect of illumination is the growth of a small shoulder at $g \approx 2.106$. The illumination does not affect the EPR signal of the Fe_4S_4 cluster because the difference spectrum, "light" *minus* "dark" (not shown), does not contain the "1.95" signal. The difference spectrum defined as c = a(light) − 0.9 × b(dark) is given in Figure 5c. The difference spectrum does not contain the "2.094" signal, indicating that after illumination the amplitude of this signal is 10% smaller. The presence of 10% residual "1.95" in spectrum c, illustrated by the dashed lines in the spectrum, reflects the fact that the "1.95" signal, being light-insensitive, was weighted in spectrum c with coefficient 0.9. The difference spectrum c shows the light-induced Mo(V) EPR signal (solid line, "2.106" signal) with the g-factors (g_z, g_y, g_x, g_{av}) = (2.106, 2.002, 1.990, 2.033). A set of minor light-induced ^{95,97}Mo-hyperfine features is observed as satellite peaks around the g_z-component of the "2.106" signal (Figure 5c′), supporting assignment of the "2.106" species to Mo(V). The "2.106" signal lacks ^{1}H-hyperfine features, and in this respect it is similar to the "2.094(D)" signal.

It was possible to monitor the kinetics of the light-induced appearance of "2.106" signal; upon illumination at 15 K, the light-induced signal reached its saturated intensity in 10 s and remained stable in the dark. If the illuminated sample

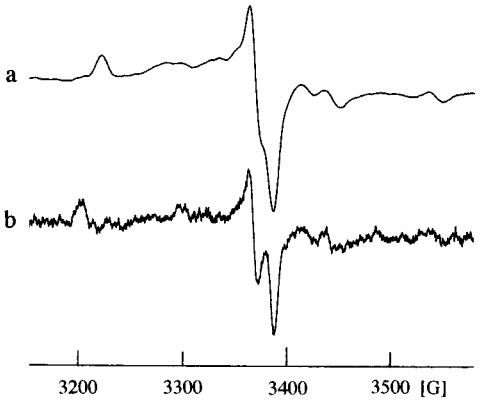

FIGURE 6: Effect of low-temperature illumination on EPR signals of ^{2}H-formate treated FDH(Se). Spectrum a was obtained from ^{2}H-formate-treated FDH(Se) illuminated at 55 K for 40 s. Spectrum b is the difference spectrum, "(spectrum a) *minus* 0.9 × (spectrum after dark adaptation)". Spectrum b is multiplied by 8-fold. Spectra were accumulated at T = 55 K and P = 12.8 mW.

was kept in darkness at T < 50 K, the amplitude of the "2.106" signal remained unchanged for a period of time longer then 1−2 h. The signal disappeared after dark adaptation, performed by placing the sample into a bath of dry ice−ethanol for 10 min. This dark adaptation did not affect the "1.95" Fe_4S_4 signal, but restored the initial amplitude of the "2.094" signal. This reversible process could be repeated at least six times with no loss of EPR signal intensities.

Comparison of the double integrals of the "2.094" and "2.106" signals indicates that there is a one-to-one correspondence between the light-induced disappearance of the "2.094" species and growth of the "2.106" species.

Several attempts have been made to increase the extent of light-induced conversion between the "2.094" and "2.106" signals. No significant variation in conversion was detected if dark-adapted samples were illuminated at three different temperatures of 7, 15, and 40 K. At 15 K attenuation of the light intensity by 50% or extension of the illumination time from 10 to 60 s also did not affect the extent of conversion. The photoconversion was independent of pH in the range from 6.0 to 8.5.

The light-induced "2.106" signal observed in ^{2}H-formate-treated FDH(Se) is shown in Figure 6. Because the light-induced signals in ^{1}H- and ^{2}H-formate treated FDH(Se) are identical, the "2.106" species is assumed to be derived from a fraction of the "2.094" species (or "2.094(D)" species) which has lost the proton (or deuteron) upon illumination at low temperature.

To explain why only 10% of the "2.094" species is transformed by light into the "2.106" species, we assume that, in addition to photodissociation, the low-temperature illumination also initiates the reverse photoreaction. In this case, the 10% level would be determined by competition between the forward and reverse photochemical reactions. Alternatively, the small yield of the "2.094" EPR signal could be due to low penetration of light in the nonglassy frozen solution of the enzyme.

Selenium Remains Ligated to Mo(V) Following Photochemical Proton Transfer. Experiments with ^{77}Se-enriched enzyme have shown that photoconverted Mo(V) centers retain ligation to Se. The light-induced signal detected in

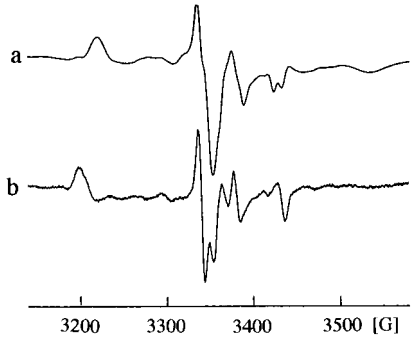

FIGURE 7: Effect of ^{77}Se-enrichment on the light-induced EPR signals of formate-treated FDH. Spectrum a was obtained from formate-treated FDH(^{77}Se) illuminated at 45.2 K for 15 s. (b) Spectrum b is the spectrum plotted as the difference "(spectrum a) *minus* 0.9 × (spectrum after dark adaptation)". Spectrum b was multiplied by 8 fold. Spectra were accumulated at $T = 45.2$ K and $P = 12.8$ mW.

formate-treated FDH(^{77}Se), the "2.106(^{77}Se)" signal, reveals distinct features derived from hyperfine interaction between Mo(V) and ^{77}Se (Figure 7).

As was also true in the case of natural isotopic abundance Se, the concentration of the light-induced "2.106(^{77}Se)" species corresponded to a 10% decrease of the "2.094(^{77}Se)" species. These spectra of the "2.094(^{77}Se)" and "2.106(^{77}Se)" species shown in parts a and b of Figure 7, respectively, have similar ^{77}Se-hyperfine values (Table 1), indicating that the light-induced transformation did not significantly alter the electronic ground state or spin density distribution of the [Mo(V)−Se]-center.

DISCUSSION

Mass-spectroscopic analysis of isotopic composition of the CO_2 gas released upon oxidation of ^{13}C-labeled formate by FDH(Se) in $H_2{}^{18}O$-enriched buffer has shown that *carbon dioxide, but not bicarbonate*, is the initial product of this reaction. Indeed, we have found that in agreement with reaction 3a and in contrast to reaction 3b, the released CO_2 gas does not incorporate the ^{18}O-label from ^{18}O-enriched water. Therefore, FDH(Se), in contrast to other molybdopterin-dependent molybdoenzymes (*19*), does not utilize a water molecule as a source of oxygen for substrate oxidation.

Involvement of "2.094" Mo(V) Species in Catalysis. The experiments with deuterated formate indicate that upon catalytic oxidation of $DCOO^-$, the nonexchangeable deuterium atom $D_f{}^+$ is transferred to the vicinity of the Mo-center and becomes water-exchangeable.

According to our model (Scheme 1) the two-electron oxidation of formate by Mo(VI) leads to formation of Mo(IV) and to release of CO_2 (reaction 1).

Here, Y^- is an unidentified proton acceptor group in the vicinity of the Mo center, and Mo(V)••H_fY denotes centers responsible for the "2.094" signal. The reactions 2 and 3 comprise two one-electron oxidation steps needed to oxidize Mo(IV)••H_fY and return the Mo center to the initial Mo(VI) state. The transfer of $H_f{}^+$ to Y^- (step 1) could include as an intermediate step the protonation of the Se ligand as proposed by Boyington et al. (1997). The first one-electron oxidation step (reaction 2) reduces the Fe_4S_4 cluster. In the absence of an exogenous acceptor, the Fe_4S_4 cluster remains

Scheme 1: Proposed Model for FDH(Se)-Catalyzed Formate Oxidation[a]

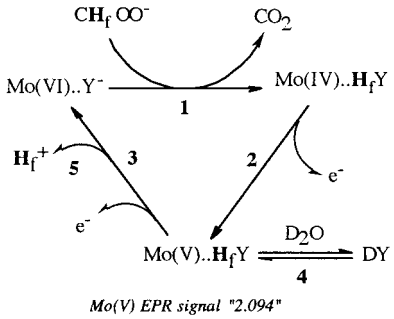

[a] Step 1: two-electron oxidation of the formate molecule by Mo(VI). Step 2: one-electron oxidation of Mo(IV) by Fe_4Se_4 centers. Step 3: one-electron oxidation of the Mo(V) centers by Fe_4S_4 centers. Step 4: slow pH-dependent exchange in D_2O-enriched buffer. Step 5: transfer of the $H_f{}^+$ from Y^- to secondary proton acceptor; the reaction is likely sensitive to the light.

in the reduced state, the second oxidation step (reaction **3**) is blocked, and, therefore, the "2.094" signal derived from the Mo(V) species is relatively stable. The intermediate state, Mo(V)••H_fY, is capable of a slow and pH−dependent $D_f{}^+/H^+$ exchange (reaction 4 in Scheme 1) which can be monitored by transformation of the ^{1}H-formate-induced "2.094" signal of FDH(Se) in D_2O into the "2.094(D)" signal.

Our mechanism is different from the two-electron formate oxidation by Mo(VI) followed by release of CO_2 and $H_f{}^+$ suggested for FDH(Se) by Heider & Bock (*37*). An essential feature of our model (Scheme 1) is that $H_f{}^+$ is not released simultaneously with formation of CO_2 but is trapped by the reduced Mo center until oxidation to the Mo(VI) state is complete (reaction 3 in Scheme 1).

Formate-Induced Inactivation of FDH(Se) by Air. Previously, formate has been shown to provoke inactivation of the FDH(Se) under anaerobic conditions (*17*). Formate was also necessary to render the enzyme susceptible to alkylation. Here, we have shown that under aerobic conditions the formate-free FDH(Se) is relatively stable. It becomes quickly inactivated by formate, indicating that the reduced Mo(V) and Mo(IV) states, but not the Mo(VI) state, are very oxygen sensitive. The lower O_2 reactivity of the Mo(VI) state is consistent with the saturated, six-coordinated ligand field, vs the five-coordinated Mo(V) and Mo(IV) centers. These coordination numbers are evident from both crystallographic and EPR data.

Se Ligand of FDH(Se). The "2.094(^{77}Se)" EPR signal provides a measure of the degree of covalent bonding between Mo(V) and Se via analysis of the hyperfine interaction with the ^{77}Se nucleus (Table 1). The isotropic part of the hyperfine interaction, $|A_{iso}|$, is in the range 16.9×10^{-4} to 36.5×10^{-4} cm^{-1}, depending on the choice of the sign of the individual tensor components which are not known from the EPR experiment. The isotropic part arises from transfer of spin density onto s-type orbitals on Se, either via direct transfer from Mo, or via s−p and s−d polarization of non-σ-type valence orbitals on Se. An appropriate estimate of the fractional spin density on Se is to compare A_{iso} to the corresponding value of atomic Se. The calculated value of $|A_{iso}|$ for atomic Se is 671.1×10^{-4} cm^{-1} (*38*). Hence, the unpaired electron in FDH(Se) is found in a molecular orbital composed of approximately 3.7 or 8.1%

Scheme 2: Light-Induced Transformation of the Mo(V) Centers[a]

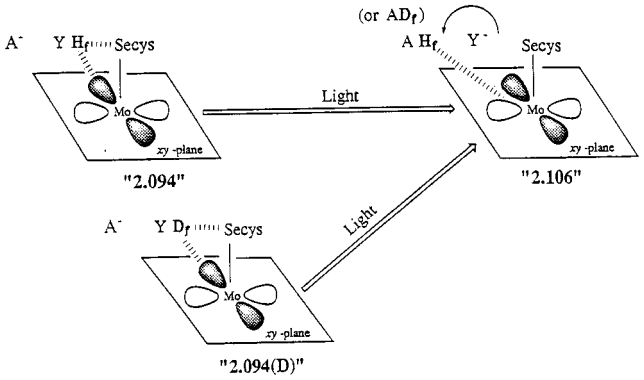

[a] Panel "2.094": the $HCOO^-$-generated Mo(V) signal "2.094" reveals ^{1}H-hyperfine structure. Panel "2.094(D)": the $DCOO^-$-generated Mo(V) signal "2.094(D)" reveals no ^{1}H-hyperfine structure. Panel "2.106": the line shape of the light-induced Mo(V) EPR signal "2.106" does not depend on whether or not the original Mo(V) signal "2.094" was generated by ^{2}H- or ^{1}H-formate.

atomic 4s(Se) orbital character. The Se p-orbital character of the valence molecular orbital is estimated similarly from the dipolar part of the ^{77}Se hyperfine interaction. For atomic ^{77}Se the $|A^d|$ value is 328.3×10^{-4} cm^{-1} (*38*), whereas $|A^d|$ for the "2.094" form of FDH(^{77}Se) ranges from 43.7×10^{-4} to 63.1×10^{-4} cm^{-1} (again depending on the choice of sign for the tensor components). This indicates that the 4p(Se) character of the valence molecular orbital in the ground state of FDH(Se) is equal to 13.3 or 19.3%. Either of these values clearly indicate that there is extensive covalent character to the Mo−Se bond. The covalency of the Mo−Se bond was estimated to be large, and from 17 to 27% of the unpaired electron spin density resides in the valence 4s and 4p selenium orbitals.

Location of the Formate-Derived Proton H_f^+. 1. Effect of the Low-Temperature Illumination on the ^{1}H Hyperfine Interaction Between H_f^+ and Mo(V). According to our model, illumination of the Mo(V) center of formate-treated FDH(Se) induces reversible transfer of the proton H_f^+ (or D_f^+) away from the Mo(V) center to a distant proton-acceptor group A^-, as shown in Scheme 2.

An increase in distance between H_f^+ (or D_f^+) and Mo(V) upon light-induced translocation of the proton (deuteron) weakens the hyperfine interaction; therefore, we expect no difference between the "2.106" signal obtained after illumination of ^{1}H-formate versus ^{2}H-formate-treated FDH(Se). This is the result we observed.

There is an alternative explanation for the disappearance of ^{1}H-hyperfine features after the photoconversion of the "2.094" species into the "2.106" species. It is possible that the low-temperature illumination does not dissociate the H_f^+ proton from the Mo center but instead affects some other site, resulting in rearrangement of the electron density around the Mo center. If the electronic ground state of the light-induced "2.106" species is not favorable for an effective ^{1}H hyperfine interaction, the ^{1}H hyperfine values would be below a limit where they could be detected by EPR.

Monitoring of ^{77}Se-hf features of the Mo(V)-center before and after illumination would be an extremely sensitive probe for the ground state of this paramagnetic species. This approach was recently used for monitoring of the photoinduced rearrangement of the electron density around the Ni−C center of [NiFeSe]-hydrogenase from *Methanococcus voltae* (*34*, *39*). It was shown that low-temperature photodissociation of the hydrogen ligand from the Ni center leads to a dramatic transformation of $A(^{77}Se)$ values, (A_{zz}, A_{yy}, A_{xx}), from (5.3, 1.5, 1.0 mT) to (3.8, 4.7, 4.3 mT), indicating rearrangement of spin density around the Ni(I) center.

In the case of FDH(Se) the light-driven conversion of the "2.094" species into the "2.106" species has little effect on the ^{77}Se hyperfine values (Table 1) and, therefore, on the electronic ground state. This means that the disappearance of the ^1H_f-hyperfine features results from the light-induced transfer of the H_f^+ away from the Mo(V) center, rather than from rearrangement of the ligands bound to the central ion.

2. Proton Acceptor Group Y^- Is Not a Ligand to Mo. Investigation of the light-related phenomena indicates that H_f^+ is not involved in protonation of direct ligands to Mo(V) centers. Indeed, if H_fY is a ligand to the Mo(V) ion, we expect that the photodissociation of H_f^+ would dramatically affect the electron structure of the Mo(V) center, its ^{77}Se-hyperfine values and *g*-factors. For example, deprotonation of [MoO(*cis*-SH)L] (where LH = *N*,*N*′-dimethyl-*N*,*N*′-bis(2-mercaptophenyl)-1,2-diaminoethane) affects dramatically the ^{33}S-hyperfine-values (A_{zz}, A_{yy}, A_{xx}) changing them from (8.5×10^{-4}, 10.1×10^{-4}, 11.4×10^{-4} cm^{-1}) to (3.8×10^{-4}, 21.5×10^{-4}, 7.2×10^{-4} cm^{-1}) (*40*). Deprotonation also changes the *g*-values of this oxo−Mo(V) model compound (g_z, g_y, g_x) from (2.0165, 1.9336, 1.8885) to (2.0155, 1.9598, 1.9523).

In our case, the illumination likely induces phototransfer of H_f^+ to a secondary proton-acceptor group A^-, increasing Mo−H_f^+ separation and decreasing the ^1H_f-hyperfine interaction with the central ion

$$\underset{\text{"2.094 (^{77}Se)"}}{^{77}\text{Se}-\text{Mo(V)}\cdot\cdot\text{YH}_f} + \text{A}^- \xrightarrow{\text{light}} \underset{\text{"2.106 (^{77}Se)"}}{^{77}\text{Se}-\text{Mo(V)}\cdot\cdot\text{Y}^-} + \text{AH}_f \quad (4a)$$

The increase of the Mo−H_f^+ separation could also be due to photoisomerization of the proton acceptor group resulting in the movement of the protonated group YH_f away from the Mo(V) center.

$$\underset{\text{"2.094 (^{77}Se)"}}{^{77}\text{Se}-\text{Mo(V)}\cdot\cdot\text{YH}_f} \xrightarrow{\text{light}} \underset{\text{"2.106 (^{77}Se)"}}{^{77}\text{Se}-\text{Mo(V)}\cdots\cdots\text{YH}_f} \quad (4b)$$

A Minimal Structure for the Mo(V) Centers. The evidence presented here and summarized below indicates that the Mo(V) state of FDH(Se) closely resembles the square pyramidal Mo(IV) center; it likely retains four *cis*-dithiolene sulfurs and the Se atom as ligands and does not accommodate a sixth ligand.

(a) No evidence is found for HO^-, HS^-, or HN-terminal ligands to Mo(V). Indeed, the largest ^{1}H-hyperfine splittings of 7.3×10^{-3} cm^{-1} characteristic of the "2.094" species is derived from a relatively remote group, YH_f, shown not to be a direct ligand to Mo(V). The presence of equatorial OH^- or SH^- terminal ligands to the Mo(V) would result in additional ^{1}H-hyperfine splittings expected in the range of $(10-20) \times 10^{-3}$ cm^{-1} (*33*, *40*−*42*). Such splittings were never observed in FDH(Se).

(b) The absence of an oxo-ligand to the Mo(V) center was demonstrated by a Mo-EXAFS study of FDH(Se) (*23*). In our EPR experiments we did not observe ^{17}O hyperfine interactions, even after the formate-treated FDH(Se) sample was diluted in $H_2{}^{17}O$-enriched buffer and stored for 24 h at 5 °C.

(c) The Mo(V) "2.094" EPR signal could be induced not only by formate but also by sodium dithionite. This implies that the formate molecule is not a ligand to Mo and its C-proton does not account for observable ^1H hyperfine splittings, except if H_f^+ is transferred to group Y^- as described above. All these data taken together suggest that oxidation of Mo(IV) to Mo(V) does not add a new ligand but does retain coordination by Se and four S atoms as ligands to Mo.

Although the Mo(V) center does not contain an oxo atom as a ligand to Mo, the symmetry of its **g**- and **A**(^{95,97}Mo)-tensors (see Table 1) is close to that observed for square-pyramidal MoO^{3+} complexes with sulfur-containing ligands. In these model compounds the oxo atom contributes the strongest ligand field vs the S ligands thereby stabilizing the d_{xy} orbital on Mo(V) as the lowest orbital (*43*−*46*). The square pyramidal ligand field and Se coordination cause several of the observed properties of the d_{xy} ground state, including (a) close to axial symmetry of the **g**-tensor with a g_z value greater than 2.00, (b) close to axial symmetry of the ^{95,97}Mo hyperfine tensor ($A_z > 2A_x \approx 2A_y$) with decreased isotropic ^{95,97}Mo hyperfine values compared to oxo−Mo-(V) compounds containing only oxygen type ligands (*47*), and (c) approximate collinearity of the *z* -axes of the **g**- and ^{95,97}Mo hyperfine tensors. All these features are also characteristic of the Mo(V) "2.094" EPR signal, Table 1.

The similarity of the EPR properties of the "2.094" and MoO^{3+} complexes with sulfur-containing ligands indicates that the Se atom is a "strong" ligand, like the oxo ligand, and dictates the d_{xy}-character of the ground electronic state of the 2.094" species (*33*, *40*, *41*, *44*, *48*, *49*). Interestingly, replacement of the terminal oxo atom in $[HB(Me_2pz)_3]$-$MoOCl_2$ by a sulfur atom, Mo═S, does not dramatically change the *g* factors and the ^{95,97}Mo hf values of the Mo(V) EPR signal (*50*). Apparently, an apical S atom is able to imitate the strong ligand field of the oxo group. The sparse number of model Mo(V)−Se compounds does not allow extension of this hypothesis to the case of terminal Se ligands. ^{77}Se hyperfine values are known only for one Se−Mo model compound, $[MoO(^{77}SePh)_4]^-$, in which Mo(V) is coordinated to four selenium atoms (*33*).

Proximity of the YH_f Group to the Se Ligand. H_f^+ is not involved in protonation of a direct ligand to the Mo(V) center, implying that estimation of the Mo−H_f^+ distance could be evaluated based on the point dipole−dipole interaction model (*51*). The model suggests that the unpaired electron density on this proton, estimated from $A_{iso}(^1H) = (A_{xx} + A_{yy} + A_{zz})/3$, is small and requires a certain relation between the principal values of the **A**(H^1) tensor, $A_{ii} \neq A_{jj} = A_{kk}$, where *i*, *j*, *k* are *x*, *y* or *z*. The $|A_{iso}|$ value depends on the choice of sign for each of A(H^1) tensor components, which are not known, and hence four different $|A_{iso}|$ values could be imagined, Table 3.

Table 3: Dependence of $|A_{iso}(^1H)|$ on Signs of A(^1H) Values[a]

cases	A_z	A_y	A_x	$\lvert A_{iso}\rvert$
I[b]	2.5	6.3	7.0	5.3
II[b]	−2.5	6.3	7.0	3.6
III[c]	2.5	−6.3	7.0	1.07
IV[c]	2.5	6.3	−7.0	0.6

[a] Hyperfine splittings are given in 10^{-4} cm^{-1}. [b] The $|A_{iso}|$ is too large to account for interaction with a distant proton. [c] The nonaxial **A**(^1H)-tensor does not fit to the point dipole model.

Cases I and II have to be omitted because the corresponding $|A(^1H)_{iso}|$ values of 5.3×10^{-4} and 3.6×10^{-4} cm^{-1} are too large to be characteristic of unpaired electron density on a distant proton. Indeed, they are fairly close to the range from 7×10^{-4} to 14×10^{-4} cm^{-1}, reported for $|A(^1H)_{iso}|$ values of the model oxo− and non-oxo−Mo(V) compounds with protonated oxygen, sulfur, or nitrogen σ-ligands (*33*, *40*, *41*, *52*, *53*). We were not able to find in the literature a model Mo(V) compound with well-characterized $|A(^1H)_{iso}|$ values from distant protons. Only those belonging to σ-ligands to Mo were found. Two values of 0.25×10^{-4} cm^{-1} and 0.1×10^{-4} cm^{-1} were reported for $VO(H_2O)_5{}^{2+}$, which were assigned to water molecules bond to the axial and equatorial sites, respectively (*33*, *54*−*57*). Although the $|A(^1H)_{iso}|$ value of 0.6×10^{-4} cm^{-1} (case IV) fits best to the distant proton, the corresponding A(^1H)-tensor is essentially non axial (Table 3, case IV). To explain this nonaxial hyperfine tensor for H_f^+, $A_{xx} \neq A_{yy} \neq A_{zz}$, we propose that H_f^+ is involved in magnetic dipole−dipole interaction with the unpaired electron spin density on both the Mo and Se atoms. The Se atom carries from 17 to 27% of the unpaired electron density.

The recent crystallographic study provides a potential clue to the identity of the group Y^-. The imidazole ring of the His141 residue is located close to the Se atom and potentially could form a hydrogen bond with this element. Moreover, the previously determined pH dependence of the catalytic activity of both the native and mutant forms of FDH (pK_a = 6.8) are consistent with the involvement of an essential histidine in catalysis (*9*, *24*).

We suggest that under the in vitro conditions employed, where electron flow is not limited by the terminal acceptor of electrons, the energy released upon oxidation of Mo(V) centers by the Fe_4S_4 is used for deprotonation of the basic His141 residue and transfer of H_f^+ against the thermodynamic potential into buffer solution. Under our catalytic conditions, where excess BV is present, the half-reaction Mo-(IV) → Mo(VI) accounts for release of the proton, as shown in Scheme 3.

Photoinduced proton transfer to a remote site A^- or photoisomerization, perhaps by rotation of the imidazole ring, could account for the significant light-induced decrease of the ^1H-hyperfine tensor. A significant movement of the His141 residue was observed in the crystal structures of oxidized and reduced forms of FDH(Se) from Mo(VI) to Mo(IV), (*6*).

Before the atomic map of the FDH(Se) became available, the sulfur atoms of the dithiolene ligands to Mo were considered as feasible candidates for the proton accepting group Y^-. The X-ray data for the Mo(VI) and Mo(IV) oxidation states indicate that the reduced Mo(IV) center retains coordination with all four sulfur atoms of the dithiolene ligands, which is not expected if one of equatorial sulfur atoms becomes protonated.

Scheme 3: Proposed Sequence of Redox Reactions Leading to Oxidation of Formate in the Presence of Benzyl Viologen (BV)

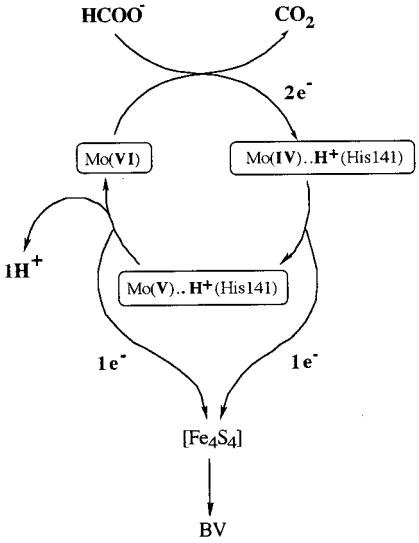

Scheme 4: Proposed Sequence of Proton-Transfer Reactions Coupled to Formate Oxidation at Room Temperature (Steps 1−5)[a]

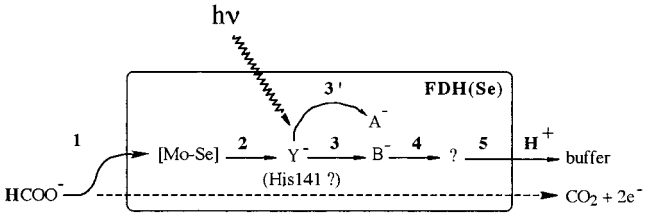

[a] The existence of the primary and secondary proton-accepting groups Y^- and A^-, respectively, was demonstrated by EPR spectroscopy, the proton-accepting B^- is suggested to function in channeling of the proton from Y^- to buffer. Electron transfer reactions are shown by the dashed line.

Proposed Chain of Proton-Carrier Groups in the FDH-(Se). The proposed sequence of proton-transfer reactions via the proton carriers Y^- and A^- is shown in Scheme 4.

In our future studies we intend to identify the chemical nature of the group A^- using ^1H ENDOR and ESEEM spectroscopies to monitor the expected weak ^1H hyperfine coupling of Mo(V) to the distant proton site AH. This approach has been successful in monitoring the light-induced proton translocation that occurs in hydrogenase (*35*).

The B^- group is a hypothetical protein residue with the physiological role of accepting protons from group Y^-. The group provides a temporary site for protons transferred out to solution (step 3, Scheme 4).

We propose eq 5a as the initial reversible chemical equilibrium in formate oxidation by FDH(Se), on the basis of data obtained from a kinetic study of formate oxidation (*24*) and based on our findings that the product is CO_2 and that the reduced enzyme binds the formate proton. The

$$FDH_{ox}\{Y^-\} + H_f\,COO^- \overset{K_{eq} \approx 0.68}{\rightleftharpoons} FDH_{red}\{H_fY\} + CO_2 \quad (5a)$$

equilibrium constant K_{eq} for the reaction is 0.68 (*24*), implying that essentially no free energy change occurs upon the release of CO_2 or its reduction to formate at the active site. The next step, eq 5b, is what drives this unfavorable step to completion. This step includes the release of the

$$FDH_{red}\{H_fY\} + 2BV \rightleftharpoons FDH_{ox}\{Y^-\} + 2BV^- + H_f^+ \quad (5b)$$

trapped proton and the reoxidation of the $FDH(Se)_{red}$.

According to this interpretation the oxidation of $FDH(Se)_{red}$ by a terminal acceptor of electrons provides the free energy needed for the transfer of H_f^+ into solution against a thermodynamic potential. The latter step involves extraction of H_f^+ from the proton accepting group Y^- (with high pK_A) into solution and most probably arises from a decrease in the pK_A of YH owing to Mo(IV) → Mo(VI) oxidation step of the Mo−Se center, which is in close physical proximity to Y^-. We suggest that this mechanism of proton release from FDH(Se) may play a physiological role in delivery of the formate proton H_f^+ to hydrogenase 3, which is the natural terminal acceptor of electrons for FDH(Se) (*8*).

ACKNOWLEDGMENT

We are thankful to Prof. Robert Scott for sharing with us the results of EXAFS study of FDH(Se), to Prof. Steven Bernasek and Ms. Karen Shafer for help in performing mass-spectroscopic experiments, to Dr. Michael Poston for interest in our work, and to Dr. David Grahame for help in preparation of FDH(Se) samples and for fruitful discussions.

REFERENCES

1. Spiro, T. G., Ed. (1985) *Molybdenum enzymes*, John Wiley & Sons, New York.
2. Rajagopalan, K. V., and Johnson, J. L. (1992) *J. Biol. Chem. 267*, 10199−10202.
3. Stiefel, E. I. (1993) in *Molybdenum enzymes, cofactors, and model systems.* (Stiefel, E. I., Coucouvanis, D., and Newton, W. E., Eds.) pp 1−19, ACS Symposium Series 535, American Chemical Society, Washington, DC.
4. Romao, M. J., Archer, M., Moura, I., Moura, J. J. G., LeGall, J., Engh, R., Schneider, M., Hof, P., and Huber, R. (1995) *Science 270*, 1170−1176.
5. Schindelin, H. S., Kisker, C., Hilton, J., Rajagopalan, K. V., and Rees, D. C. (1996) *Science 272*, 1615−1621.
6. Boyington, J. C., Gladyshev, V. N., Khangulov, S. V., Stadtman, T. C., and Sun, P. D. (1997) *Science 275*, 1305−1308.
7. Chan, M. K., Mukund, S., Kletzin, A., Adams, M. W. W., and Rees, D. C. (1995) *Science 267*, 1463−1469.
8. Sawers, G. (1994) *Antonie-Van-Leeuwenhoek 66*, 57−88.
9. Axley, M. J., Grahame, D. A., and Stadtman, T. C. (1990) *J. Biol. Chem. 265*, 18213−18218.
10. Stadtman, T. C., Davis, J. N., Ching, W.-M., Zinoni, F., and Bock, A. (1991) *BioFactors 3*, 21−27.
11. Zinoni, F., Birkmann, A., Stadtman, T. C., and Bock A. (1986) *Proc. Natl. Acad. Sci. U.S.A. 83*, 4650−4654.
12. Gladyshev, V. N., and Lecchi, P. (1996) *BioFactors 5*, 93−97.
13. Gladyshev, V. N., Khangulov, S. V., and Stadtman, T. C. (1994) *Proc. Natl. Acad. Sci. U.S.A. 91*, 232−236.
14. Gladyshev, V. N., Khangulov, S. V., Axley, M. J., and Stadtman, T. C. (1994) *Proc. Natl. Acad. Sci. U.S.A. 91*, 7708−7711.
15. Dilworth, G. L. (1982) *Arch. Biochem. Biophys 219*, 30−38.
16. Dilworth, G. L. (1983) *Arch. Biochem. Biophys. 221*, 565−569.
17. Axley, M. J., Bock, A., and Stadtman, T. C. (1991) *Proc. Natl. Acad. Sci. U.S.A. 88*, 8450−8454.

18. Zinoni, F., Birkmann, A., Leinfelder, W., and Bock, A. (1987) *Proc. Natl. Acad. Sci. U.S.A. 84*, 3156−60.
19. Holm, R. (1987) *Chem. Rev. 87*, 1401.
20. Hille, R. (1996) *Chem. Rev. 96*, 2757−2816.
21. Schultz, B. E., Gheller, S. F., Muetterties, M. C., Scott, M. J., and Holm, R. H. (1993) *J. Am. Chem. Soc. 115*, 2714−2722.
22. Schultz, B. E., and Holm, R. H. (1993) *Inorg. Chem. 32*, 4244−4248.
23. George, G. N., Colangelo, C. M., Dong, J., Scott, R. A., Khangulov, S. V., Gladyshev, V. N., and Stadtman, T. C. (1998) *J. Am. Chem. Soc.* (in press).
24. Axley, M. J., and Grahame, D. A. (1990) *J. Biol. Chem. 265*, 13731−13736.
25. Poston, J. M., Stadtman, T. C., and Stadtman, E. R. (1971) *Methods Enzymol. 22*, 49−54.
26. Hung, W.-H. (1992) Ph.D. Dissertation, Princeton University, Princeton, NJ.
27. Gladyshev, V. N., Boyington, J. C., Khangulov, S. V., Grahame D. A., Stadtman, T. C., and Sun, P. D. (1996) *J. Biol. Chem. 271*, 8095−8100.
28. Nilges, M. J. (1979) Ph.D. Dissertation, University of Illinos, Urbana, IL.
29. Aasa, R., and Vanngard T. (1975) *J. Magn. Reson. 19*, 308.
30. Orme-Johnson, W. H., Hansen, R. E., Beinert, H., Tsibris, J. C. M., Bartholomaus, R. C., and Gunsalus, I. C. (1968) *Proc. Natl. Acad. Sci. U.S.A. 60*, 368−315.
31. Mukai, K., Huang, J. J., and Kimura, T. (1973) *Biochem. Biophys. Res. Com. 50*, 105−110.
32. Bertini, I., Ciurli, S., Dikiy, A., and Luchinat, C. (1993) *J. Am. Chem. Soc. 115*, 1202.
33. Hanson, G. R., Wilson, G. L., Bailey, T. D., Pilbrow, J. R., and Wedd, A. G. (1987) *J. Am. Chem. Soc. 109*, 2609−2616.
34. Sorgenfrei, O., Klein, A., and Albracht, S. P. J. (1993) *FEBS 332*, 291−297.
35. Whitehead, J. P., Gurbiel, R. J., Bagyinka, C., Hoffman, B. M., and Maroney, M. J. (1993) *J. Am. Chem. Soc. 115*, 5629−5635.
36. Medina, M., Hatchikian, E. C., and Cammack R. (1996) *Biochim. Biophys. Acta 1275*, 227−236.
37. Heider, J., and Bock, A. (1993) *Adv. Microb. Physiol. 35*, 71−109.
38. Weltner, W., Jr. (1983) *Magnetic Atoms and Molecules*, pp 341−348, Dover Publication, Inc., New York.
39. Sorgenfrei, O., Duin, E. C., Klein, A., and Albracht, S. P. J. (1996) *J. Biol. Chem. 271*, 23799−23806.
40. Wilson, G. L., Greenwood, R. J., Pilbrow, J. R., Spence, J. T., and Wedd, A. G. (1991) *J. Am. Chem. Soc. 113*, 6803−6812.
41. Dowerah, D., Spence, J. T., Singh, R., Wedd, A. G., Wilson, G. L., Farchione, F., Enemark, J. H., Kristofzski, J., and Bruck, M. (1987) *J. Am. Chem. Soc. 109*, 5655−5665.
42. Greenwood, R. J., Wilson, G. L., Pilbrow, J. R., and Wedd, A. G. (1993) *J. Am. Chem. Soc. 115*, 5385−5392.
43. Ballhausen, C. J., and Gray, H. B. (1962) *Inorg. Chem. 1*, 111−122.
44. Gray, H. B., and Hare, C. R. (1962) *Inorg. Chem 1*, 363−368.
45. Kon, H., and Sharpless, N. E. (1965) *J. Chem. Phys. 42*, 906−909.
46. DeArmond, K., Garrett, B. B., and Gutowsky, H. S. (1965) *J. Chem. Phys. 42*, 1019−1025.
47. Marov, I. N., Belyaeva, V. K., Ermakov, A. N., and Dubrov, Y. N. (1969) *Russ. J. Inorg. Chem. 14*, 1391−1402.
48. Hanson, G. R., Brunette, A. A., McDonell, A. C., Murray, K. S., and Wedd, A., G. (1981) *J. Am. Chem. Soc. 103*, 1953−1959.
49. Dubrov, Y. N., Marov, I. N., Belyaeva, V. K., and Ermakov, A., N. (1972) *Russ. J. Inorg. Chem. 17*, 1278−1283.
50. Young, C. G., Enemark, J. H., Collison, D., and Mabbs, F. E. (1987) *Inorg. Chem.* 2925−2927.
51. Goodman, B. A., and Raynor, J. B. (1970) in *Advances in Inorganic Chemistry and Radiochemistry 13* (Emeleus, H. J., and Sharpe, A. G., Eds.) pp 135−362, Academic Press, New York.
52. Pariyadath, N., Newton, W. E., and Stiefel, E. I. (1976) *J. Am. Chem. Soc. 98*, 5388−5389.
53. Cleland, W. E., Barnhart, K. M., Yamanouchi, K., Collision, D., Mabbs, F. E., Ortega, R. B., and Enamark, J. H. (1987) *Inorg. Chem. 26*, 1017−1025.
54. Vigee, G., and Selbin, J. (1968) *J. Inorg. Nucl. Chem. 30*, 2273.
55. Albanese, N. F., and Chasteen, N. D. (1978) *J. Chem. Phys. 82*, 910−914.
56. Willgen, H. (1980) *J. Magn. Reson. 39*, 37−46.
57. Dikanov, S. A., Evelo, R. G., Hoff, A. J., and Tyryshkin, A. M. (1989) *Chem. Phys. Lett. 154*, 34−38.

BI972177K